minerals

MDPI

Article

Pyrochlore-Group Minerals in the Granite-Hosted Katugin Rare-Metal Deposit, Transbaikalia, Russia

Anastasia E. Starikova [1,2,*], Ekaterina P. Bazarova [3], Valentina B. Savel'eva [3], Eugene V. Sklyarov [3,4], Elena A. Khromova [5] and Sergei V. Kanakin [5]

1 V.S. Sobolev Institute of Geology and Mineralogy, Siberian Branch of the Russian Academy of Sciences, 3 Akad. Koptyug av., 630090 Novosibirsk, Russia
2 Department of Geology and Geophysics, Novosibirsk State University, 2 Pirogov st., 630090 Novosibirsk, Russia
3 Institute of the Earth's Crust, Siberian Branch of the Russian Academy of Sciences, 128 Lermontova st., 664033 Irkutsk, Russia
4 School of Engineering, Far East Federal University, 8 Sukhanov st., 690091 Vladivostok, Russia
5 Geological Institute, Siberian Branch of the Russian Academy of Sciences, 6a, Sakhjanova st., 670047 Ulan-Ude, Russia
* Correspondence: starikova@igm.nsc.ru; Tel.: +7-913-207-8362

Received: 8 May 2019; Accepted: 13 August 2019; Published: 15 August 2019

Abstract: Pyrochlore group minerals are the main raw phases in granitic rocks of the Katugin complex-ore deposit that stores Nb, Ta, Y, REE, U, Th, Zr, and cryolite. There are three main types: Primary magmatic, early postmagmatic (secondary-I), and late hydrothermal (secondary-II) pyrochlores. The primary magmatic phase is fluornatropyrochlore, which has high concentrations of Na_2O (to 10.5 wt.%), F (to 5.4 wt.%), and REE_2O_3 (to 17.3 wt.%) but also low CaO (0.6–4.3 wt.%), UO_2 (to 2.6 wt.%), ThO_2 (to 1.8 wt.%), and PbO (to 1.4 wt.%). Pyrochlore of this type is very rare in nature and is limited to a few occurrences: Rare-metal deposits of Nechalacho in syenite and nepheline syenite (Canada) and Mariupol in nepheline syenite (Ukraine). It may have crystallized synchronously with or slightly later than melanocratic minerals (aegirine, biotite, and arfvedsonite) at the late magmatic stage when Fe from the melt became bound, which hindered the crystallization of columbite. Secondary-I pyrochlore follows cracks or replaces primary pyrochlore in grain rims and is compositionally similar to the early phase, except for lower Na_2O concentrations (2.8 wt.%), relatively low F (4 wt.%), and less complete A- and Y-sites occupancy. Secondary-II pyrochlore is a product of late hydrothermal alteration, which postdated the formation of the Katugin deposit. It differs in large ranges of elements and contains minor K, Ba, Pb, Fe, and significant Si concentrations but also low Na and F. Its composition mostly falls within the field of hydro- and keno-pyrochlore.

Keywords: pyrochlore-group minerals; fluornatropyrochlore; alkaline granites; Katugin rare-metal deposit; East Transbaikalia

1. Introduction

Pyrochlore-group minerals (part of the pyrochlore supergroup of minerals) are broadly occurring in nature and are of important economic interest due to their ability to host Ta, Nb, U, and REE. They are common accessory phases in carbonatite and are often found in such lithologies as nepheline syenite, alkaline gabbro and granitoids, pegmatite, and in albite and greisen granites [1–8]. Pyrochlore minerals have diverse compositions with the general formula $A_{2-m}B_2O_{6-w}Y_{1-n}$, where A represents large cations (Na, Ca, U, Th, REE, Y, Sr, Ba, Pb, Sn, and H_2O) and site vacancies, the B-site is occupied by smaller cations (Nb, Ti, and Ta), and Y is occupied by F, OH^-, O^{2-}, and H_2O or site vacancies [9–11]. The symbols *m*, *w*, and *n* represent parameters indicating incomplete occupancy of the A, X, and Y.

The Ca/Na ratios vary considerably. Fluorcalciopyrochlore $(Ca,Na)_2Nb_2O_6F$ is the most widespread phase in the group [3,10,12]. Findings of pyrochlore with prominent Na enrichment over Ca and other cations at the A-site are very few and are limited to several rare-metal deposits hosted by the Nechalacho syenite and nepheline syenite (Canada) [13,14], the Mariupol nepheline syenite (Ukraine) [15], the Strange Lake granite (Canada) [16], and the Halzdan-Buregteg alkaline granite (West Mongolia) [17]. Fluornatropyrochlore $(Na,Pb,Ca,REE,U)_2Nb_2O_6F$ was reported as a mineral species from the Boziguoer granites (China) only in 2013 [18].

Pyrochlore is one of main ore phases in the exceptionally rich Ta-Nb-REE-Zr Katugin deposit. In spite of a long history of exploration and research at the Katugin field [19,20], the available knowledge on mineralogy of pyrochlore is insufficient to reveal its types and formation features at different stages of the ore formation process. Previous studies [19] and references therein] were restricted to pyrochlore monofractions identified according to color, habit, and other external characteristics and provided no constraints on mineral chemistry trends. Later publications on the Katugin deposit [20–23] did not give much attention to pyrochlore. This study bridges the gap by distinguishing several types of pyrochlore and tracing their crystallization sequences. Special focus is made on high-Na pyrochlore, which is of rare natural occurrence and thus remains poorly characterized.

2. Geological Setting

The Katugin deposit, extremely rich in REE, Nb, and Ta, is located in the Aldan shield, at the southern margin of the Chara-Olekma terrane near the border with terranes of the Central Asian Orogenic Belt marked by the Stanovik suture [24]. The ores are hosted by two relatively small (3 and 18 km^2) A-type alkaline granite intrusions of the Katugin complex [21,22] (Figure 1a), which were earlier interpreted as alkaline metasomatites [19,25–27]. The Western intrusion is 80% buried under a moraine and remains quite poorly documented. The Eastern intrusion (Figure 1b) is composed of three types of granites corresponding to three phases of magmatism [21,22]: Phases I, II, and III, respectively, of biotite (Bt) and biotite-riebeckite (Bt-Rbk); biotite-arfvedsonite (Bt-Arf); and arfvedsonite, aegirine-arfvedsonite and aegirine (Arf, Aeg-Arf, and Aeg) granites. Phase III granites have diverse mineralogy and lack distinct boundaries. They are joined into one phase because the Aeg, Aeg-Arf, and Arf varieties sometimes grade from one to another in a single sample. All types are medium- and fine-grained, often gneissic, leucocratic and mesocratic quartz-albite-microcline granites with variable amounts of melanocratic minerals. At the same time, some arfvedsonite and aegirine granites appear as isolated pegmatitic veins.

Biotite and biotite-riebeckite granites (phase I) have moderate or high Al contents and relatively high CaO, but contain the smallest amount of F among all granites we sampled. Biotite-arfvedsonite granites (phase II) are supersaturated with respect to alkalis, rich in CaO and Y, but poor in Na_2O and F. The ore-bearing granites of phase III are likewise supersaturated in alkalis; they have high concentrations of Na_2O and F but very low CaO, and are mostly rich in Zr, Hf, Nb, and Ta [21].

The Katugin granites host Zr, Ta-Nb-REE, and F-Al mineralization [19,20]. Zircons are present either as sporadic grains or as large clusters (to 20 vol.%) in all rocks of the intrusion. Fluoraluminate minerals include abundant cryolite (a large body on the intrusion margin and ≤3 cm globules in Aeg granites) and smaller percentages of other phases (weberite, chiolite, prosopite, pachnolite, thomsenolite, and Ba-fluoraluminates). Ta-Nb-REE phases are mainly pyrochlore, columbite-(Fe), fluorides (fluocerite-(Ce), gagarinite-(Y), tveitite-(Y), yttrofluorite) and fluorcarbonates (bastnäsite-(Ce) and parisite-(Ce)) or less often monazite-(Ce). REE fluorides and fluorcarbonates often form aggregates unevenly distributed in the rocks [23,28,29]. Other minerals include ilmenite, magnetite, and sulfides (sphalerite, galena, pyrrhotite or pyrite). Ta-Nb-REE-Zr mineralization formed at 2055 ± 7 Ma, around the time of the Katugin granite emplacement (2066 ± 6 Ma), the difference being within the scope of analytical error [24,30].

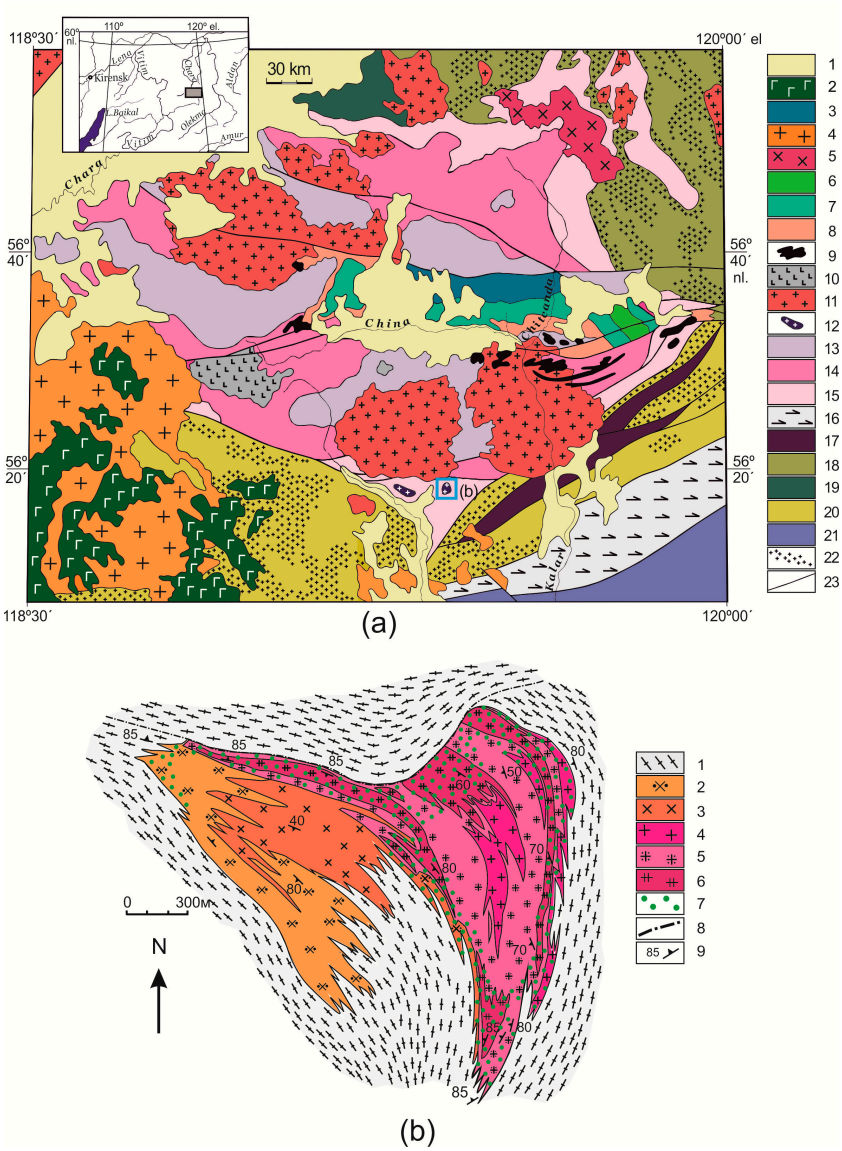

Figure 1. (**a**): Simplified geological map of the region of the Katugin granite complex, after [22,31]. 1 = Quaternary sediments; 2 = flood basalts (N_2-Q); 3 = Jurassic coal-bearing clastic sediments; 4 = granite, granodiorite, granosyenite and monzonite of the Ingamakit complex (PZ_3); 5 = nepheline syenite, granosyenite and monzonite of the Khanin complex (PZ_3); 6 = Ordovician variegated sediments; 7 = Cambrian variegated sediments; 8 = Vendian variegated sediments; 9 = gabbro-dolerite, gabbro and dolerite porphyrite of the Doros complex; 10 = layered plutons of the Chinei complex; 11 = granite of the Kodar complex; 12 = rare-metal granite of the Katugin complex; 13–15 = carbonate and clastic sediments of the Udokan supergroup: Kemen group (13), Chinei group (14), and Kodar group (15); 16 = anorthosite of the Kalar complex; 17 = low-grade metamorphic volcanic-sedimentary rocks of the Subgan complex; 18 = tonalite-trondjemite orthogneis of the Olekma complex; 19 = Chara sequence (garnet-biotite and garnet-hypersthene-biotite plagiogneiss, mafic schists, quartzite and magnetite quartzite); 20 = Kalar sequence (garnet-biotite plagiogneiss with layers and lenses of two-pyroxene mafic granulite, clac-silicate rocks, quartzite, and magnetite quartzite; 21 = metamorphic and igneous complexes of the Selenga-Stanovik superterrane in the Central Asian orogenic belt; 22 = zones of widespread Precambrian granitic rocks; 23 = faults. (**b**): Simplified geology of the Katugin granite intrusion, after [21,32]. 1 = gneiss, migmatite, blastomylonite of the Kodar group, Udokan group; 2–6 = Katugin granites of different types: biotite (2), biotite-riebeckite (3), biotite-arfvedsonite (4), arfvedsonite (5), aegirine-arfvedsonite and aegirine (6); 7 = ore-bearing granite; 8 = faults; 9 = bedding elements.

3. Materials and Methods

The analytical work was performed at the Analytical Center for Multielement and Isotope Studies of the V.S. Sobolev Institute of Geology and Mineralogy (Novosibirsk, Russia) and at the Analytical Center for Mineralogical, Geochemical, and Isotope Studies of the Geological Institute (Ulan-Ude, Russia). We analyzed pyrochlore monofractions from different types of the Katugin granites: Biotite, biotite-riebeckite, biotite-arfvedsonite, arfvedsonite, aegirine-arfvedsonite, and aegirine granites, as well as aegirine granite enriched in zircon, pyrochlore, and REE phases (the ore-rich aegirine granite). The mineral phases were identified and analyzed using a Carl Zeiss LEO-1430VP scanning electron microscope equipped with an Oxford Instruments INCAEnergy 350 energy-dispersive microanalysis system (EDS method, Analysts E.A. Khromova and S.V. Kanakin, Geological Institute, Ulan-Ude). The electron beam was operated at an accelerating voltage of 20 kV, a beam current of >0.5 nA and a count time of 50 s. Element concentrations in pyrochlores were measured on a Jeol JXA-8100 electron-microprobe analyzer (WDS method) at the Institute of Geology and Mineralogy, Novosibirsk (analyst E.N. Nigmatulina). The operation conditions were: 2 μm beam diameter, 30 nA beam current, 20 kV accelerating voltage, and 10 s count time on peak per element. The results were calibrated using the following standards: albite (Na, Al, Si); diopside (Ca); F-phlogopite (F, K, and Mg); garnet (Fe, Mn); ($LiNbO_3$ (Nb); rutile (Ti); Ta_2O_5 (Ta); zircon (Zr); UO_2 (U); ThO_2 (Th); SrSi glass (Sr); PbTe (Pb); BaSi glass (Ba); $KLaMoO_4$ (La); $LiCeWO_4$ (Ce); $CsPrMoO_4$ (Pr); $RbNdWO_4$ (Nd); $LiSmMoO_4$ (Sm); $LiGdMoO_4$ (Gd); $LiDyWO_4$ (Dy); and $Y_3Al_5O_{12}$ (Y). Detection limits were (3σ, in wt.%): 0.07 for Na, 0.06 for Al, 0.1 for Si, 0.02 for Ca, 0.09 for F, 0.02 for K, 0.04 for Mg, 0.01 for Fe, 0.02 for Mn, 0.08 for Nb, 0.04 for Ti, 0.16 for Ta, 0.15 for Zr, 0.09 for Th, 0.08 for U, 0.27 for Sr, 0.14 for Pb, 0.06 for Ba, 0.08 for La, 0.14 for Ce, 0.11 for Pr, 0.1 for Nd, 0.06 for Sm, 0.11 for Gd, 0.05 for Dy, and 0.18 for Y. The PAP program was applied for matrix correction. The error rate was less than 2 rel.% for major elements.

4. Results

Pyrochlore-group minerals are main ore phases of the Katugin rare-metal deposit common to different granitic rocks of the complex, except for Bt and Bt-Rbk granites of phase I which bear columbite-(Fe) as a predominant opaque mineral and low percentages of pyrochlore. Pyrochlore is especially abundant in phase III Aeg and Aeg-Arf granites where it occurs as round or rarely octahedral euhedral grains (≤5 mm) or as clusters and lenses, including in ore-rich zones. The pyrochlore grains are honey-yellow to almost black but most often brown (Figure 2). There are three main types of pyrochlore identified according to crystallization sequence and chemistry: Primary pyrochlore found as isolated crystals or aggregates; secondary-I pyrochlore looking darker-shaded in BSE images, which follows cracks, replaces earlier pyrochlore in grain rims, and is occasionally enclosed in zircon from Aeg-Arf granites; and the latest secondary-II in most strongly altered and deformed grain parts (Figure 2). Primary pyrochlore in Bt-Arf granites is rarely replaced by later phases but rather by aggregates of columbite, gagarinite-(Y), and bastnäsite-(Ce) (Figure 2a). Pyrochlore from Aeg, Aeg-Arf, and Arf (phase III) granites often encloses numerous veinlets or microcrystals (10 μm on average) of other minerals (bastnäsite-(Ce), gagarinite-(Y), yttrofluorite, and occasionally rutile) produced by alteration (Figure 2f). Columbite-(Fe) replaces pyrochlore in some grains. Some pyrochlores enclose cryolite, quartz, albite, feldspar, aegirine, zircon, and magnetite.

4.1. Primary Pyrochlore

The (#Nb) pyrochlore-group end-members predominate over those of microlite (#Ta) or betafite (#Ti) groups in all analyses of primary pyrochlore (Figure 3; Tables 1–3). The B-site is occupied by 1.54–1.84 apfu of Nb (#Nb—73–90 mol.%), 0.125–0.4 apfu of Ti (#Ti—7.5–23 mol.%), and up to 0.3 apfu of Ta (#Ta—0–15 mol.%). The A-site accommodates large cations of Na, REE + Y, and Ca (Figure 4), as well as U, Th and Pb (the total of the three elements in the A-site being no more than 6%). REE are mainly

represented by Ce, while HREE and Y are low. This pyrochlore contains abundant F, which occupies the Y-site (Figure 5).

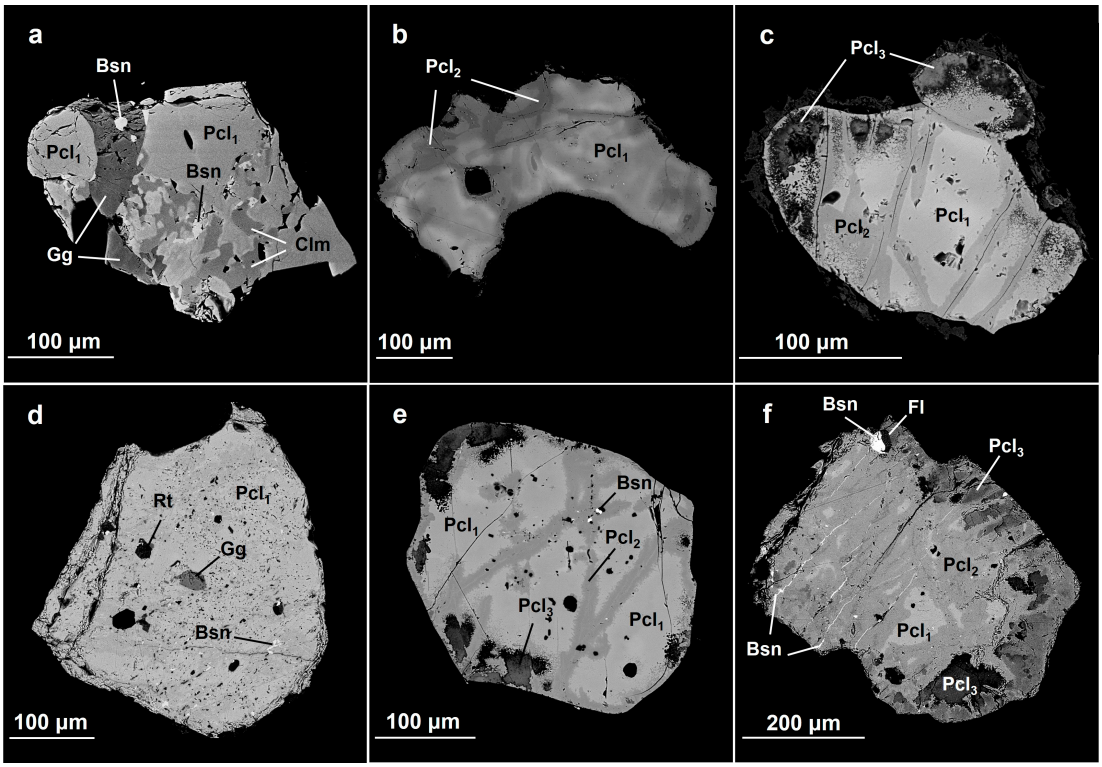

Figure 2. Pyrochlore-group minerals from the Katugin granites of different types (BSE image). (**a**,**b**): Bt-Arf granite; (**c**): Bt-Rbk granite; (**d**): Aeg-Arf granite; (**e**,**f**): Aeg granite. Mineral names are abbreviated as Bsn = bastnäsite, Clm = columbite, Fl = fluorite, Gg = gagarinite-(Y), Pcl_1 = primary pyrochlore, Pcl_2 = secondary-I pyrochlore, Pcl_3 = secondary-II pyrochlore, Rt = rutile.

Primary pyrochlore from Bt-Arf granites differs from those in other granite types and contains as much as 6.4 to 10.7 wt.% Na_2O (Figure 5; Table 1), which exceeds previously reported values from different occurrences worldwide (within 9.18 wt.% Na_2O) [14]. It is also rich in niobium (up to 62 wt.% Nb_2O_5) but has low TiO_2 of 2.4 to 3.8 wt.% (Figure 3). Some pyrochlore grains in these granites are zoned, possibly according to growth (Figure 2b), with Ta_2O_5-rich (to 15 wt.%) lighter-color zones. Ta enrichment may result from accumulation in evolving granitic melt [3]. The Bt-Arf granite-hosted pyrochlore shows the most complete cation occupancy of the A-site (1.55–2 apfu), with high REE (16.7 wt.% $LREE_2O_3$ and 1.6 wt.% $HREE_2O_3$) and 1.3 wt.% Y_2O_3 but low UO_2 (0.3–0.9 wt.%) and PbO (to 0.21 wt.%). The contents of CaO vary from 1.4 to 3.5 wt.%, with the Na/Ca ratio from 3.7 to 13 (7.1 on average). Fluorine reaches 5.34 wt.% or 1.15 apfu. The LREE/HREE and Y/Ce ratios vary from 8 to 37 and 0.04 to 0.34, the averages of 18.2 and 0.16, respectively. The general formula of this pyrochlore can be expressed as $(Na_{1.2}Ca_{0.18}LREE_{0.36}HREE_{0.04}Y_{0.03}U_{0.02}Th_{0.02})_{1.85}(Nb_{1.8}Ti_{0.15}Ta_{0.05})_2O_{5.94}F_{1.06}$.

Primary pyrochlores from Bt, Bt-Rbk granites of phase I and Arf, Aeg-Arf and Aeg granites of phase III are compositionally similar (Tables 2 and 3) and differ from that in the ore-rich Aeg granite. The latter hosts pyrochlore with low CaO (0.63–0.85 wt.%) but relatively high $HREE_2O_3$ (2.4 wt.%) and Y_2O_3 (4 wt.%) (Table 3), which has the highest ratios of Na/Ca (10.2–15.2) and Y/Ce (0.72–0.81) but lowest LREE/HREE (6.5–7.7) compared to the counterparts from other granite types (Figure 5e).

The betafite component (#Ti) with 3.75 to 8 wt.% TiO_2 increases progressively from 9.8% in Bt and Bt-Rbk granites to 19.9% in Aeg granite, while pyrochlore component (#Nb) decreases correspondingly (Figure 3); the microlite component (#Ta) varies from 2 to 4.4 wt.% Ta_2O_5. The A occupancy in pyrochlores from Bt, Bt-Rbk, Arf, Aeg-Arf, and Aeg granites varies from 1

to 1.55 apfu while Na does not exceed 0.95 apfu (8.1 wt.% Na_2O) being on average 0.83 apfu (6.5 wt.% Na_2O). CaO in some pyrochlores from Bt, Bt-Rbk and Aeg-Arf granites has a large range, including within the same sample (2 to 5.5 wt.%; Na/Ca = 2–7.2), but is quite stable (2.3–2.8 wt.%; Na/Ca = 3.7–5) in pyrochlore from all aegirine granites (Figure 5). The latter pyrochlore also has high REE_2O_3: 15–16 wt.% (LREE/HREE = 16–21; Y/Ce = 0.08–0.23) against 10–14.5 wt.% REE_2O_3 (LREE/HREE = 10–19; Y/Ce = 0.1–0.25) in pyrochlores from other granite types. UO_2, ThO_2 and PbO do not exceed 2.6 wt.%, 1.8 wt.%, and 1.4 wt.%, respectively. F is 3.6 to 5.5 wt.% (4.6 wt.% on average).

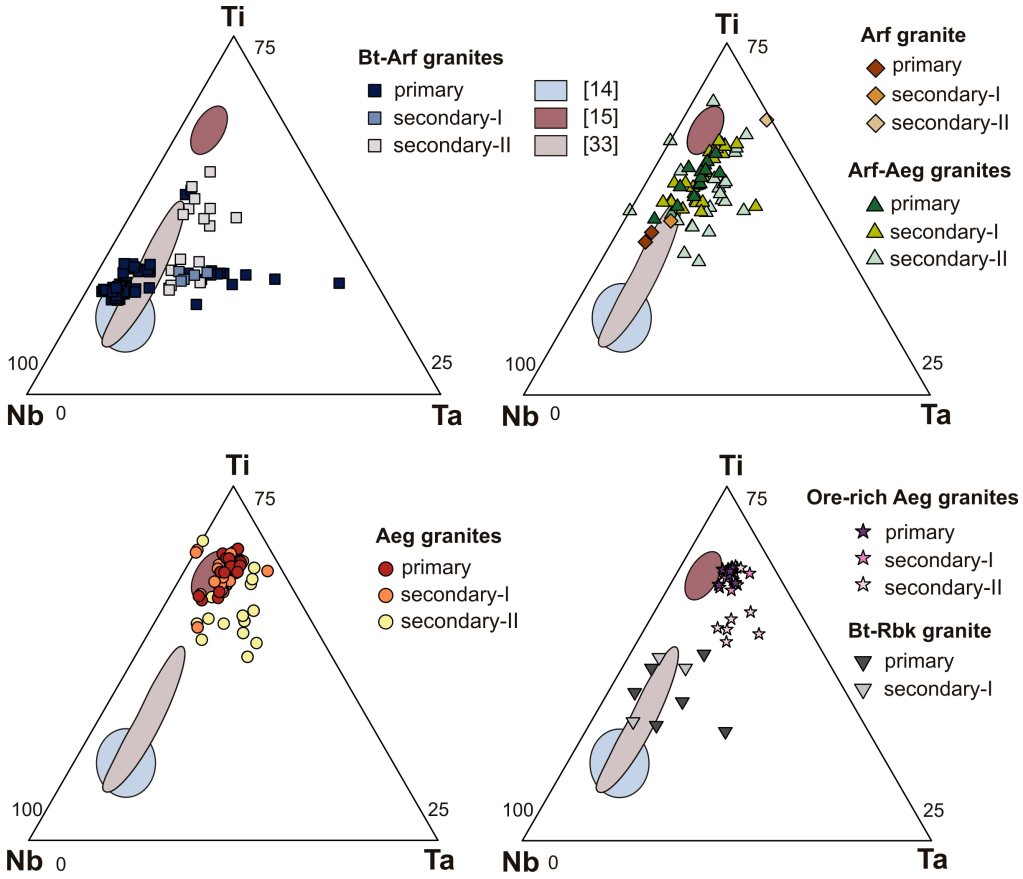

Figure 3. Ternary classification diagrams (B-site) for pyrochlore-group minerals from the Katugin granites. [14], [15], [33] = fields of fluornatropyrochlores from literature [14,15,33], respectively.

4.2. Secondary-I Pyrochlore

Secondary-I pyrochlore differs from the primary variety in low contents of Na_2O (1–4.5 wt.%, 2.8 wt.% on average), lower F (2–5 wt.%, 4 wt.% on average), and less complete occupancy of the A- and Y-sites (Tables 1–3; Figures 4 and 5). Other cations have concentrations commensurate with those in early pyrochlore.

4.3. Secondary-II Pyrochlore

Secondary-II pyrochlore differs compositionally from the earlier pyrochlores. It has large ranges of both major and trace elements (Tables 1–3; Figures 3–5) and analytical totals that are notably below 100%. Unlike the earlier counterparts, it contains minor amounts of K_2O (up to 2.3 wt.%), BaO (to 3 wt.%), PbO (to 2.5 wt.%), and Fe_2O_3 (to 0.6 wt.%) and relatively high SiO_2 (to 9.2 wt.%) (Figures 5f and 6). The contents of ThO_2 (to 2.1 wt.%) and UO_2 (to 5.6 wt.%) are higher while REE_2O_3, CaO, Na_2O, Nb_2O_5, Ta_2O_5, and F are markedly lower relative to those in primary and secondary-I

pyrochlores. Most of secondary-II pyrochlore samples fall in the field of hydro- or kenopyrochlore (Figure 4).

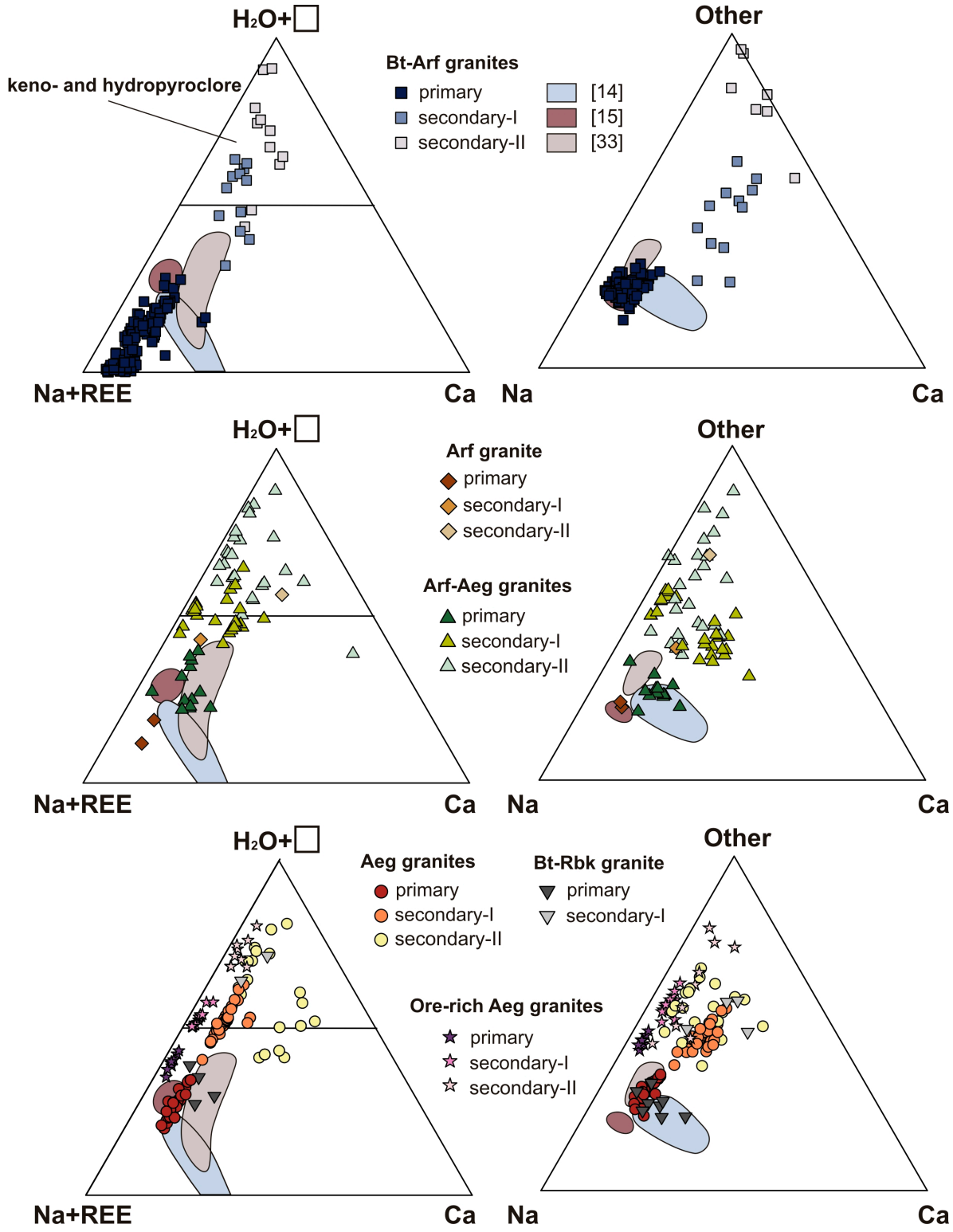

Figure 4. Ternary classification diagrams (A-site) for pyrochlore-group minerals from the Katugin granites. In the Ca-Na + REE-H_2O + □ diagrams, Ca stands also for other divalent cations (Mn, Pb, Sr, Ba); Na+REE stands also for Y, U, Th, and K; □ is vacancy.

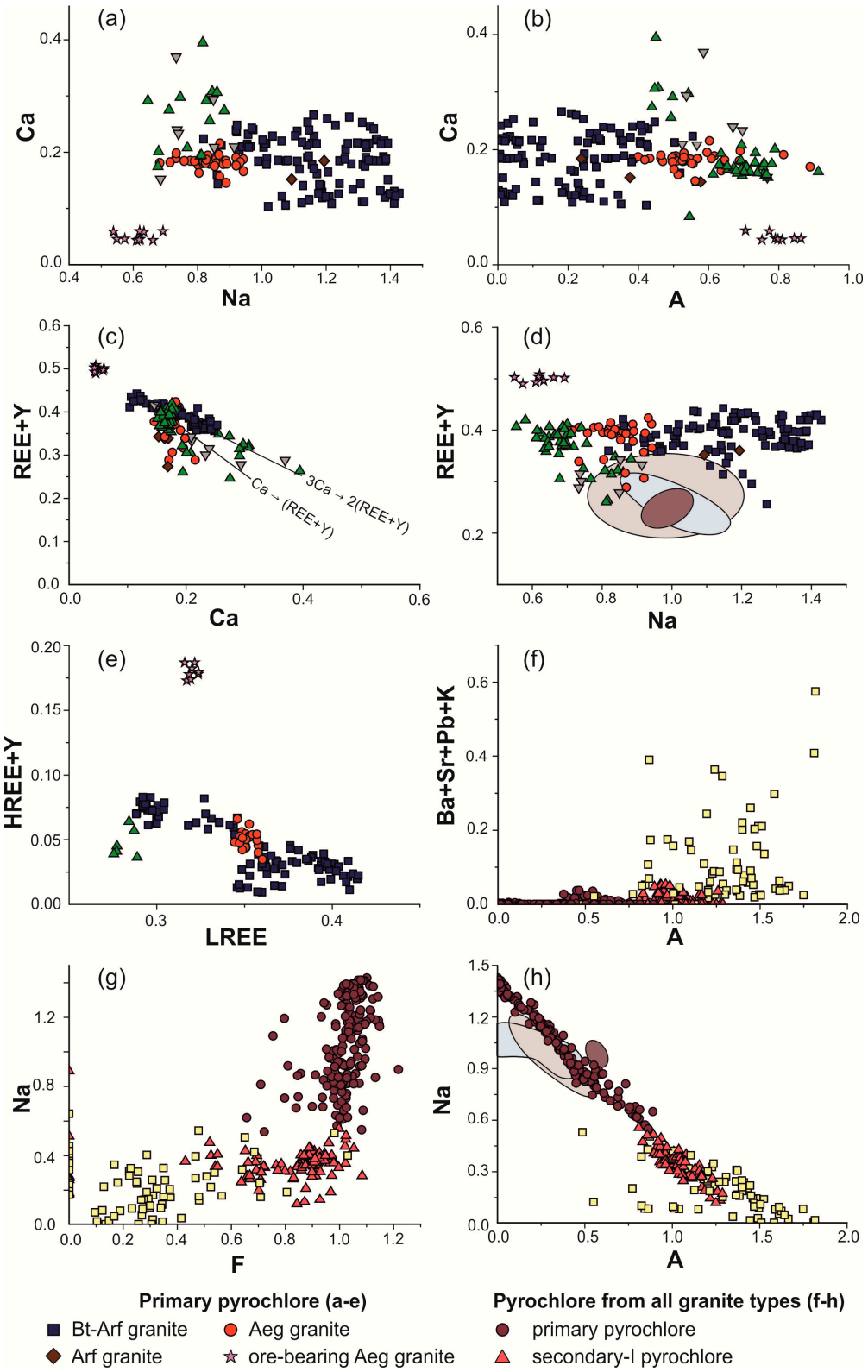

Figure 5. Binary diagrams (apfu) for pyrochlore-group minerals from the Katugin granites. A = vacancy or H_2O at the A-site. The HREE+Y/LREE diagram includes only WDS data.

Table 1. Chemistry (wt.%) of pyrochlore-group minerals from the Katugin biotite-arfvedsonite granite (WDS analyses).

Constituent	I						II		III		
	1	**2**	**3**	**4**	**5**	**6**	**n = 12**	**sd**	**n = 8**	**min**	**max**
Na_2O	10.46	9.18	8.60	9.95	7.22	6.77	2.25	1.24	1.11	3.07	1.26
K_2O	bdl	bdl	bdl	bdl	bdl	bdl	bdl	0.02	0.54	0.06	1.31
CaO	1.68	1.66	3.23	3.47	2.78	3.19	3.53	1.26	2.44	0.19	3.52
SrO	bdl	bdl	bdl	bdl	bdl	bdl	0.09	0.17	0.96	0.28	1.55
BaO	bdl	bdl	bdl	bdl	bdl	bdl	0.15	0.23	1.90	bdl	2.94
PbO	bdl	bdl	bdl	bdl	0.11	0.11	0.54	0.75	1.28	bdl	2.31
La_2O_3	2.00	2.14	1.24	1.42	2.18	2.08	2.00	0.56	0.86	0.34	1.75
Ce_2O_3	8.30	8.72	6.15	5.97	7.81	7.92	7.45	1.23	4.36	1.84	6.55
Pr_2O_3	1.18	1.06	0.90	0.77	0.88	0.85	0.78	0.11	0.38	bdl	0.68
Nd_2O_3	3.52	3.51	3.2	2.78	2.56	2.53	2.39	0.45	1.11	0.53	1.91
Sm_2O_3	0.75	0.83	1.02	0.83	0.50	0.47	0.49	0.13	0.26	bdl	0.46
Gd_2O_3	0.45	0.30	0.82	0.81	0.38	0.28	0.29	0.15	0.15	bdl	0.28
Dy_2O_3	0.25	0.24	0.60	0.65	0.24	0.17	0.14	0.08	bdl	bdl	bdl
Y_2O_3	0.49	0.53	0.90	1.29	bdl	0.56	0.19	0.24	0.09	bdl	0.30
ThO_2	1.30	1.51	0.84	0.69	0.81	0.82	1.35	0.69	1.26	0.73	1.63
UO_2	0.37	0.39	0.70	0.66	1.49	1.56	1.76	0.18	2.19	1.68	3.06
Al_2O_3	bdl	Bdl	bdl	bdl	bdl	bdl	bdl	-	0.17	bdl	0.30
SiO_2	bdl	Bdl	bdl	bdl	bdl	bdl	0.02	0.06	4.47	1.49	7.40
TiO_2	2.84	2.79	3.05	2.67	2.85	3.05	4.20	1.19	3.66	2.64	4.56
Nb_2O_5	59.75	61.24	62.21	61.86	49.32	52.87	55.71	1.67	50.06	46.13	55.38
Ta_2O_5	2.64	2.06	2.20	2.27	15.23	11.51	4.54	1.42	5.03	4.39	6.13
F	4.83	4.94	4.89	4.91	4.52	4.81	4.26	0.46	2.28	0.63	3.91
Total	101.01	101.08	100.54	101.00	98.88	99.54	92.13		84.87		
O_2=F	2.03	2.08	2.06	2.07	1.90	2.02	1.79		0.96		
Total	98.98	99.01	98.48	98.94	96.98	97.52	90.33		83.91*		
ΣREE_2O_3	16.45	16.79	13.93	13.23	14.55	14.30	13.53		7.12		
Na	1.354	1.174	1.075	1.261	0.979	0.895	0.295		0.136		
K	-	-	-	-	-	-	-		0.044		
Ca	0.120	0.117	0.223	0.243	0.208	0.233	0.256		0.165		
Sr	-	-	-	-	-	-	0.003		0.035		
Ba	-	-	-	-	-	-	0.004		0.047		
Pb	-	-	-	-	0.002	0.002	0.010		0.022		
LREE	0.382	0.389	0.292	0.279	0.355	0.344	0.323		0.161		
HREE	0.015	0.012	0.030	0.031	0.014	0.010	0.009		0.003		
Y	0.017	0.019	0.031	0.045	-	0.020	0.007		0.003		
Th	0.020	0.023	0.012	0.010	0.013	0.013	0.021		0.018		
U	0.006	0.006	0.010	0.010	0.023	0.024	0.027		0.031		
ΣA	1.914	1.739	1.673	1.880	1.595	1.540	0.954		0.62		
Al	-	-	-	-	-	-	-		0.013		
Si	-	-	-	-	-	-	0.001		0.283		
Ti	0.143	0.138	0.148	0.131	0.150	0.156	0.213		0.174		
Nb	1.809	1.825	1.813	1.828	1.560	1.630	1.702		1.433		
Ta	0.048	0.037	0.039	0.041	0.290	0.213	0.084		0.087		
ΣB	2.000	2.000	2.000	2.000	2.000	2.000	2.000		2.000		
F	1.018	1.028	0.996	1.016	1.001	1.037	0.911		0.456		
#Nb	90.47	91.24	90.68	91.42	78.01	81.51	85.15		84.61		
#Ti	7.13	6.91	7.39	6.56	7.50	7.82	10.67		10.27		
#Ta	2.40	1.85	1.93	2.02	14.49	10.67	4.178		5.12		

Note: 1–4 = pyrochlores without visible zoning; 5, 6 = rims in zoned pyrochlores. n is number of analyses; sd is standard deviation; numerals I, II, III correspond to primary, secondary-I and secondary-II pyrochlores, bdl is below detection limit. For compositionally variable secondary-II pyrochlore, minimum (min) and maximum (max) element contents are given instead of standard deviations. Formula is based on 2 cations at B-site. #Nb, #Ti, #Ta are pyrochlore, betafite, and microlite end-member components (mol.%), respectively. *The total also includes 0.07 wt.% Fe_2O_3 and 0.19 ZrO_2.

Table 2. Chemistry (wt.%) of pyrochlore-group minerals from the Katugin biotite and biotite-riebeckite granites (1) and arfvedsonite aegirine-arfvedsonite granites (2).

Constituent	1				2						
	I		II		I		II		III		
	n = 7	sd	n = 3	sd	n = 11	sd	n = 21	sd	n = 23	min	max
Na_2O	6.61	0.63	2.66	1.56	6.91	0.96	3.00	0.50	1.90	0.20	3.83
K_2O	bdl	-	bdl	-	bdl	-	bdl	0.02	0.45	0.15	1.17
CaO	3.71	1.05	2.85	0.44	3.56	1.28	2.52	1.69	1.34	0.39	3.06
SrO	bdl	-	bdl	-	0.13	0.27	0.29	0.30	0.42	bdl	1.40
BaO	bdl	-	bdl	-	bdl	-	0.06	0.15	0.81	bdl	2.89
PbO	bdl	-	bdl	-	0.94	0.48	0.57	0.45	1.04	0.25	2.52
La_2O_3	2.19	0.35	2.15	0.45	1.44	0.64	1.43	0.33	0.78	0.26	1.59
Ce_2O_3	8.55	1.32	8.80	0.93	6.85	0.77	7.11	0.66	5.49	3.10	7.92
Pr_2O_3	0.36	0.59	bdl	-	0.73	0.11	0.77	0.18	0.50	0.24	0.77
Nd_2O_3	3.29	0.31	3.06	0.28	2.58	0.42	2.55	0.38	1.35	0.61	2.32
Sm_2O_3	bdl	-	bdl	-	0.69	0.15	0.76	0.18	0.43	0.16	0.69
Gd_2O_3	bdl	-	bdl	-	0.58	0.20	0.70	0.32	0.32	bdl	0.66
Dy_2O_3	bdl	-	bdl	-	0.40	0.26	0.58	0.43	0.43	bdl	1.18
Y_2O_3	bdl	-	bdl	-	1.10	0.93	1.81	1.52	0.71	bdl	1.99
ThO_2	bdl	-	bdl	-	1.00	0.43	1.03	0.45	1.05	0.20	2.06
UO_2	1.64	1.18	2.16	0.56	1.86	0.06	1.90	0.28	2.61	1.53	5.50
Al_2O_3	bdl	-	bdl	-	bdl	-	bdl	-	0.23	bdl	0.64
Fe_2O_3	bdl	-	bdl	-	bdl	0.01	bdl	0.01	0.17	bdl	2.05
SiO_2	bdl	-	1.51	0.23	bdl	-	0.02	0.07	5.47	2.34	9.24
TiO_2	4.33	0.87	4.3	0.97	5.92	0.91	6.27	0.82	5.04	2.81	6.54
ZrO_2	bdl	-	bdl	-	0.02	0.05	0.01	0.04	0.37	bdl	1.53
Nb_2O_5	58.08	2.56	55.06	1.15	54.26	1.13	53.21	0.84	47.56	41.76	54.36
Ta_2O_5	4.38	2.53	2.96	1.08	3.27	0.59	3.75	0.51	4.74	3.24	6.83
F	4.88	0.51	2.98	1.78	4.55	0.53	3.79	1.17	1.85	bdl	3.27
Total	98.10		88.51		96.79		92.13		85.05		
O_2=F	2.05		1.25		1.91		1.60		0.78		
Total	96.05		87.25		94.88		90.53		84.27		
ΣREE_2O_3	14.43		14.02		13.28		13.90		9.23		
Na	0.837		0.339		0.897		0.390		0.226		
K	-		-		-		-		0.035		
Ca	0.260		0.201		0.256		0.181		0.088		
Sr	-		-		0.005		0.011		0.015		
Ba	-		-		-		0.002		0.019		
Pb	-		-		0.017		0.010		0.017		
LREE	0.342		0.336		0.299		0.307		0.190		
HREE	-		-		0.022		0.028		0.015		
Y	-		-		0.039		0.065		0.023		
Th	-		-		0.015		0.016		0.015		
U	0.024		0.032		0.028		0.028		0.036		
ΣA	1.463		0.907		1.577		1.038		0.679		
Al	-		-		-		-		0.017		
Fe^{3+}	-		-		-		-		0.008		
Si	-		0.099		-		0.001		0.334		
Ti	0.231		0.213		0.298		0.316		0.237		
Zr	-		-		0.001		-		0.011		
Nb	1.591		1.635		1.642		1.613		1.315		
Ta	0.073		0.053		0.059		0.068		0.079		
ΣB	2.000		2.000		2.000		2.000		2.000		
F	1.005		0.619		0.963		0.804		0.357		
#Nb	90.18	90.97	90.43	91.07	77.26	81.00	85.15		84.61		
#Nb	85.49		86.02		82.13		80.75		80.65		
#Ti	10.64		11.20		14.90		15.83		14.52		

Note: 1 = EDS analyses; 2 = WDS analyses. Other symbols as in Table 1.

Table 3. Chemistry (wt.%) of pyrochlore-group minerals from the Katugin aegirine granites (WDS analyses).

Constituent	1							2		
	I		II		III			I	II	III
	n = 42	sd	n = 46	sd	n = 23	min	max	n = 8	n = 14	n = 9
Na_2O	6.67	0.63	2.68	0.55	2.03	0.63	3.96	4.93	2.83	1.47
K_2O	bdl	-	bdl	-	0.46	bdl	1.67	bdl	bdl	0.72
CaO	2.68	0.21	2.61	0.20	1.56	bdl	2.98	0.69	0.68	0.81
MnO	bdl	-	bdl	-	1.24	bdl	2.09	bdl	bdl	bdl
SrO	0.04	0.10	0.05	0.11	0.02	bdl	0.17	bdl	0.03	0.02
PbO	0.57	0.10	0.60	0.14	0.98	bdl	3.52	0.18	0.23	0.86
La_2O_3	2.22	0.67	2.18	0.61	0.68	bdl	1.45	1.48	1.44	0.73
Ce_2O_3	8.36	0.56	8.26	0.45	4.1	bdl	7.67	7.42	7.18	5.60
Pr_2O_3	0.93	0.08	0.91	0.07	0.45	0.15	0.82	0.82	0.83	0.52
Nd_2O_3	2.89	0.34	2.80	0.28	1.23	0.47	2.14	2.88	2.76	1.42
Sm_2O_3	0.75	0.05	0.74	0.05	0.34	0.12	0.57	1.01	0.99	0.48
Gd_2O_3	0.54	0.05	0.51	0.07	0.26	bdl	0.46	1.13	1.08	0.55
Dy_2O_3	0.35	0.04	0.35	0.06	0.21	bdl	0.40	1.11	1.05	0.72
Y_2O_3	0.88	0.18	0.82	0.12	0.06	bdl	0.50	3.84	3.70	0.96
ThO_2	1.12	0.11	1.13	0.10	1.39	0.80	1.91	0.75	0.70	0.93
UO_2	1.85	0.11	1.84	0.24	2.46	bdl	5.62	1.77	1.75	2.78
Al_2O_3	bdl	-	bdl	-	0.18	bdl	0.38	bdl	bdl	0.35
Fe_2O_3	bdl	-	bdl	-	1.18	bdl	2.89	bdl	bdl	0.05
SiO_2	0.04	0.19	0.08	0.27	5.07	1.23	9.05	bdl	bdl	5.50
TiO_2	7.57	0.87	7.49	0.73	6.47	4.52	10.01	7.76	7.51	5.94
ZrO_2	bdl	-	bdl	-	bdl	bdl	bdl	bdl	bdl	0.31
Nb_2O_5	54.21	2.76	53.31	2.48	50.66	40.22	63.26	53.22	51.75	47.97
Ta_2O_5	3.08	0.47	2.77	0.05	4.23	bdl	10.91	3.53	3.56	4.96
F	4.78	0.54	3.74	1.45	1.00	0.55	3.55	4.94	4.00	1.44
Total	99.54		92.88		85.86			97.45	92.06	85.10
O_2=F	2.01		1.58		0.42			2.08	1.69	0.61
Total	97.53		91.30		84.51			95.37	90.37	84.49
ΣREE_2O_3	16.05		15.75		7.18			15.84	15.33	10.01
Na	0.833		0.339		0.231			0.620	0.365	0.170
K	-		-		0.034			-	-	0.055
Ca	0.185		0.183		0.098			0.048	0.049	0.052
Mn	-		-		0.122			-	-	-
Sr	0.002		0.002		0.001			-	0.001	0.001
Pb	0.010		0.011		0.015			0.003	0.004	0.014
LREE	0.355		0.354		0.143			0.320	0.319	0.190
HREE	0.019		0.018		0.009			0.047	0.046	0.025
Y	0.030		0.028		0.002			0.132	0.131	0.031
Th	0.016		0.017		0.019			0.011	0.011	0.013
U	0.027		0.027		0.032			0.026	0.026	0.037
ΣA	1.477		0.979		0.706			1.207	0.952	0.586
Al	-		-		0.012			-	-	0.025
Fe^{3+}	-		-		0.051			-	-	0.002
Si	0.003		0.005		0.289			-	-	0.329
Ti	0.366		0.369		0.277			0.378	0.376	0.268
Nb	1.577		1.577		1.305			1.560	1.559	1.295
Ta	0.054		0.049		0.066			0.062	0.065	0.082
ΣB	2.000		2.000		2.000			2.000	2.000	2.000
F	0.973		0.774		0.181			1.014	0.844	0.272
#Nb	78.96		79.05		79.05			77.98	77.96	78.86
#Ti	18.34		18.48		18.48			18.90	18.81	16.23
#Ta	2.70		2.47		2.47			3.11	3.23	4.91

Note: 1 = pyrochlore-group minerals from ordinary (1) and ore-rich (2) aegirine granites. Other symbols as in Table 1.

5. Discussion

5.1. Comparison with Fluornatropyrochlore from Other Occurrences

Pyrochlores of three types from the Katugin granites differ notably in their chemistry and show quite large ranges of some element concentrations. Primary pyrochlore, with high Na and F concentrations and low Ca, is of special interest and can be classified as fluornatropyrochlore. The latter has been rarely found in natural occurrence [4–6,13–17] and became a registered mineral species as late as in 2013 [18]. In this respect, it is pertinent to compare the Katugin pyrochlore with its counterparts that are known from other places.

Fluornatropyrochlore from the Boziguoer rare-metal granites in China (the first finding of this mineral) differs from the samples we analyzed in higher concentrations of PbO (to 16.17 wt.%) and UO_2 (5.8–7.5 wt.%) [18,33] and much lower Na_2O (5.5–8.5 wt.%) (Figures 4 and 5) at quite high Na/Ca ratios of 4.1–6.6. The F contents in the Boziguoer pyrochlore range within 4.6–7.1 wt.% or 1.25 to 1.63 apfu [33] exceeding the common value of 1 apfu at least by a factor of ~1.5 requires additional explanation, as overestimation may lead to notable structure distortion.

Fluornatropyrochlores with the highest Na contents were reported from the Nechalacho [13,14] and Mariupol [15] syenites and nepheline syenites but the pyrochlores from both occurrences have Na_2O lower than in those from the Katugin Bt-Arf granites (7–9.18 wt.% Na_2O against an average of 9.4 wt.%, respectively). On the other hand, they have UO_2 (within 1.1 wt.%), ThO_2 (≤1.6 wt.%) and PbO (≤0.5 wt.%) as low as in the Katugin pyrochlores.

All other published fluornatropyrochlore compositions with high Na/Ca ratios have predominant components with 0.78 to 0.93 #Nb (Figure 3), but their REE_2O_3 contents (mainly LREE) are much lower (to 13.4 wt.%) than in the Katugin pyrochlores (Figure 5d). Low Y/Ce ratios (0.04–0.32) in all Katugin pyrochlores we analyzed, except for those from ore-bearing Aeg granite (Y/Ce to 0.8), are similar to the ratios reported for their counterparts from other occurrences.

5.2. Isomorphism in the Katugin Pyrochlores

Judging by their chemistry, pyrochlore-group minerals are prone to extensive homo- and heterovalent isomorphic substitutions at all sites, which follow hardly decipherable scenarios. Incorporation of REE^{3+}, U^{4+} and Th^{4+} in primary pyrochlore may balance the excess of Na with respect to the ideal neutral formula $NaCaNb_2O_6F$, at complete X occupancy. Therefore, the substitution in A-site is expected to proceed as $2Ca^{2+} \rightarrow Na^+ + REE^{3+}$; $3Ca^{2+} \rightarrow 2Na^+ + U^{4+}(Th^{4+})$. However, Na in primary pyrochlore correlates neither with Ca nor with REE + Y (Figure 5a,d), but the latter shows distinct inverse correlation with Ca (Figure 5c). The substitution apparently followed the scenario $3^{A}Ca^{2+} \rightarrow 2^{A}REE^{3+}$ for the pyrochlores hosted by Bt-Arf granites and for some of those from Aeg-Arf granites, but 1 REE substituted for 1 Ca in the Bt-Rbk and Aeg granites. In the absence of other correlations with Ca, it remains unclear how the arising positive charge could be balanced. Most likely, several substitutions worked jointly.

Na correlates inversely with the A-site vacancy (r = −0.85 to −0.99) (Figure 5h), and its poor correlation with F (Figure 5g) is inconsistent with the $^{A}Na^+ + {}^{Y}F^- \rightarrow$ A+Y substitution, where A and Y are the respective site vacancies. The high inverse Na-A correlation may result from incorporation of the (OH)-group in the X-site or H_3O^+ in the A-site by the $^{A}Na^+ + {}^{X}O^{2-} \rightarrow A + {}^{X}(OH)^-$ and $Na^+ \rightarrow H_3O^+$ or by some more intricate substitution. The contents of $^{X}OH^-/AH_3O^+$ in a charge-balanced formula should be 0.24 apfu on average for primary pyrochlore from Bt-Arf granite and as high as 0.78 apfu for primary pyrochlores from other granite types, as estimated proceeding from the total cation charge provided that all Y occupancy is by F^-.

Secondary-I pyrochlore which differs from the early phase only in lower Na and F contents formed by alteration of primary fluornatropyrochlore mainly by the $^{A}Na^+ + {}^{Y}F^- \rightarrow A + Y$; $^{A}Na^+ + {}^{X}O^{2-} \rightarrow A + {}^{X}(OH)^-$ and $^{A}Na^+ \rightarrow {}^{A}H_3O^+$ substitutions. The ratio $^{X}OH^-/{}^{A}H_3O^+$ in this pyrochlore is 1.09 apfu on average.

Secondary-II pyrochlore shows maximum Na, Ca and F leaching at incomplete A occupancy, with the $Na^+ + F^- \rightarrow A + Y$ or, possibly, also $Ca^{2+} + 2F^- \rightarrow A + 2Y$ substitutions. The total cation charge is 0.7–2.1 less than that at complete X occupancy by oxygen. In addition to the $^{A}Na^+ + {}^{X}O^{2-} \rightarrow A + {}^{X}(OH)^-$ and $Na^+ \rightarrow H_3O^+$ substitutions inferred for two other types of pyrochlore, the substitution in the latest pyrochlore may be $^{A}Ca^{2+} + {}^{X}O^{2-} \rightarrow A + X$ (A and X are the respective vacancies).

Si in Secondary-II Pyrochlore

Silicon is a common component in pyrochlore-group minerals. Minor amounts of Si may incorporate in the B-site, as mentioned in a recent nomenclature paper [10]. However, there were reports of "silicified" pyrochlore with up to 9.31 wt.%, 11.51 wt.%, 13 wt.% and 15 wt.% SiO_2 [15,34–36]. The Si mode of occurrence in the pyrochlore structure remains a subject of discussions, and several solutions have been suggested. The radius of Si^{4+} is much smaller than that of B-site cations and large amounts of Si^{4+} cannot incorporate without significantly distorting the mineral structure. The existence of "silicified" pyrochlore was attributed to the presence of Si-bearing mineral microinclusions [37], amorphous or dispersed Si [38], or submicronic intergrowths with komarovite $(H,Ca,Na)_2(Nb,Ti)_2Si_2O_{10}(OH,F)_2$ [35]. On the other hand, M. Dumanska-Slowik et al. [15] showed metamictization to be the key factor that allows incorporation of Si as it causes damage to A- and B-sites. They [15] failed to detect Si at the B-site though, but Bonazzi et al. [34] confirmed the presence of Si and estimated that 30–50% of Si in "silicified" pyrochlore was incorporated in the B-site, where it replaced Nb and Ta, and partly in the structure portion damaged by radiation.

The Katugin secondary-II pyrochlore contains up to 9.24 wt.% SiO_2 and apparently lacks Si-bearing mineral inclusions (all analyses were made for homogeneous grain portions). Furthermore, SiO_2 shows significant inverse correlation with TiO_2 ($r = -0.85$) and a weaker correlation with Nb_2O_5 ($r = -0.65$), which indicates that Si occupies the B-site (Figure 6). This pyrochlore contains more U, Th and Pb than both earlier phases and appears to be strongly metamictized. Thus, some amount of Si in the Katugin "silicified" pyrochlore may occupy the B-site and some Si may be incorporated in the α-damaged part, in the same way as suggested in reference [34].

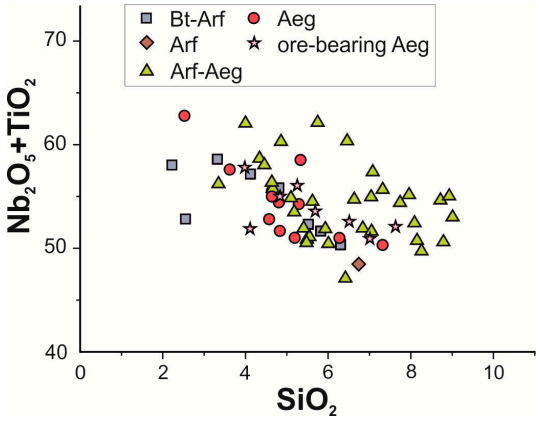

Figure 6. SiO_2 vs $Nb_2O_5 + TiO_2$ diagram (wt.%) for secondary-II pyrochlore from the Katugin granites.

5.3. Genesis of Different Pyrochlore Types in the Katugin Rare-Metal Deposit

It was previously found out that REE phases in the Katugin alkaline granites crystallized after main rock-forming minerals (feldspar and quartz) from residual melt rich in Fe, Na, Zr, Nb, Ta, Zn, Sn and volatiles (F, CO_2, P, S, and H_2O) [28]. Primary pyrochlore is the earliest REE phase. Crystallization of pyrochlore was synchronous with or slightly postdating the formation of melanocratic phases (aegirine, biotite, and arfvedsonite). Fe extracted from the melt became bound in the melanocratic minerals, which hindered the crystallization of columbite [2]. The unusual chemistry of primary pyrochlore with very high Na/Ca may be controlled by the composition of the host Katugin granites

supersaturated with alkalis and F, rich in REE + Y, and depleted in Ca [21]. However, the chemical peculiarity of pyrochlore must be due more to high concentrations of REE than to high Na/Ca ratios, given that Na-richest pyrochlores occur in Bt-Arf granites containing more Ca than the Aeg, Aeg-Arf, and Arf granites. Rare earths are incorporated into the structure of pyrochlore (the earliest REE phase), while Na replaces Ca for charge balance.

Secondary-I pyrochlore likely formed at the early postmagmatic stage in the evolution of the Katugin complex, judging by its presence, along with primary pyrochlore, as inclusions in zircon which was previously interpreted as magmatic or early postmagmatic [24,39].

The presence of pyrochlores with almost leached Ca, Na, and F, as well as partial incorporation of K, Ba, and Sr, were attributed to weathering [1,40,41]. However, these pyrochlores show neither significant Si enrichment nor Nb depletion. The origin of "silicified" pyrochlore was explained in the context of high-temperature hydrothermal activity [15] and metasomatism [35]. The Katugin rocks are not much weathered, though they include widespread products of hydrothermal alteration of cryolite (weberite, pachnolite, etc.) and Ba-aluminosilicates [42]. Secondary-II pyrochlore was possibly formed by hydrothermal alteration at the late postmagmatic stage, judging by relatively high Ba contents. Yet, there is no evidence that it happened during the formation of the ore deposit.

6. Conclusions

Pyrochlore group minerals are the main raw phases in granitic rocks of the Katugin rare-metal deposit. They are of three main types: primary magmatic pyrochlore occurring as round or less often octahedral grains, early postmagmatic (secondary-I) pyrochlore following cracks or replacing primary pyrochlore in grain rims, and late hydrothermal (secondary-II) pyrochlore that replaces the two earlier types.

The primary magmatic phase is fluornatropyrochlore very rare in nature, with a Na/Ca ratio of 3.7 to 15.2. Some primary pyrochlores we discovered have exceptionally high Na_2O contents (up to 10.7 wt.%), higher than those from any previously reported occurrences. The Katugin pyrochlores have greater REE_2O_3 enrichment (up to 17.3 wt.%) than high-Na pyrochlores from other known occurrences but similar low Y/Ce ratios (0.04–0.34). The total of other cations at the A-site (U, Th and Pb) does not exceed 6%. The Katugin fluornatropyrochlore is compositionally close to those from Nechalacho, Canada, and Mariupol (Ukraine) syenite and nepheline syenite. Primary pyrochlore owes its unusual chemistry more likely to high REE^{3+} activity during crystallization than to high alkalinity of the host granite. In this case, the arising positive charge became balanced by the $2\,{}^{A}Ca^{2+} \rightarrow {}^{A}Na^{+} + {}^{A}REE^{3+}$ substitution. The substitutions in primary pyrochlore most often followed the ${}^{A}Na^{+} + {}^{X}O^{2-} \rightarrow A + {}^{X}(OH)^{-}$, ${}^{A}Na^{+} \rightarrow {}^{A}H_3O^{+}$, and $3\,{}^{A}Ca^{2+} \rightarrow 2\,{}^{A}REE^{3+}$ scenarios.

Secondary-I pyrochlore may have replaced the primary phase during the cooling of the intrusion, at the postmagmatic stage. Compared to the primary pyrochlore, it has lower concentrations of Na_2O (1 to 4.5 wt.%, 2.8 wt.% on average) and F (2 to 5 wt.%, 4 wt.% on average) and less complete occupancy of the A and Y sites, while the contents of other components are similar. Thus, secondary-I pyrochlore replaced that of primary by the ${}^{A}Na^{+} + {}^{Y}F^{-} \rightarrow A + Y$; ${}^{A}Na^{+} + {}^{X}O^{2-} \rightarrow A + {}^{X}(OH)^{-}$ or ${}^{A}Na^{+} \rightarrow {}^{A}H_3O^{+}$ substitutions.

Secondary-II pyrochlore appears to be a product of late hydrothermal alteration of early fluoraluminate phases (mainly cryolite) and postdated the formation of two other pyrochlore types. It shows large ranges of major oxides (REE_2O_3, CaO, Na_2O, Nb_2O_5, Ta_2O_5), contains minor amounts of K_2O, BaO, PbO, and Fe_2O_3, and has totals notably below 100%. This pyrochlore type is remarkable because it has a relatively high enrichment in Si (up to 9.2 wt.% SiO_2) which is partly incorporated in the B-site and partly in the α-damaged portion of the structure. The composition of secondary-II pyrochlore mostly falls within the field of hydro- and kenopyrochlore and results from the $Na^{+} + F^{-} \rightarrow A + Y$, $Ca^{+} + 2F^{-} \rightarrow A + 2Y$, ${}^{A}Na^{+} + {}^{X}O^{2-} \rightarrow A + {}^{X}(OH)^{-}$, $Na^{+} \rightarrow H_3O^{+}$, and ${}^{A}Ca^{2+} + {}^{X}O^{2-} \rightarrow A + X$ substitutions (A, Y and X are vacancies at the respective sites).

Author Contributions: Conceptualization, A.E.S. and E.P.B.; formal analysis, A.E.S., E.A.K. and S.V.K.; investigation, A.E.S., E.P.B.; resources, A.E.S., E.P.B. and E.V.S.; writing—original draft preparation, A.E.S. and E.P.B; writing—review and editing, A.E.S., E.V.S. and V.B.S; visualization, A.E.S.

Funding: This research was funded by the Russian Foundation for Basic Research (Project 16-35-60054 mol_a_dk). Scanning Electron Microscopy was funded by the Russian Science Foundation (Project 14-17-00325). WDS was carried out as part of government assignment to the V.S. Sobolev Institute of Geology and Mineralogy.

Acknowledgments: We thank T. Perepelova and V.V. Sharygin for assistance in manuscript preparation. Thoughtful comments by four anonymous reviewers on this manuscript are gratefully acknowledged.

Conflicts of Interest: Authors declare no conflict of interest.

References

1. Nasraoui, M.; Bilal, E. Pyrochlores from the Lueshe carbonatite complex (Democratic Republic of Congo): A geochemical record of different alteration stages. *J. Asian Earth Sci.* **2000**, *18*, 237–251. [CrossRef]
2. Ogunleye, P.O.; Garba, I.; Ike, E.C. Factors contributing to enrichment and crystallization of niobium in pyrochlore in the Kaffo albite arfvedsonite granite, Ririwai Complex, Younger Granites province of Nigeria. *J. Asian Earth Sci.* **2006**, *44*, 372–382. [CrossRef]
3. Yaroshevskii, A.A.; Bagdasarov, Y.A. Geochemical diversity of minerals of the pyrochlore group. *Geochem. Int.* **2008**, *46*, 1245–1266. [CrossRef]
4. Guarino, V.; de' Gennaro, R.; Melluso, L.; Ruberti, E.; Azzone, R.G. The transition from miaskitic to agpaitic rocks as marked by the accessory mineral assemblages, in the Passa Quatro alkaline complex (southeastern Brazil). *Can. Mineral.* **2019**, *57*, 1–23. [CrossRef]
5. Guarino, V.; Wu, F.Y.; Melluso, L.; Gomes, C.B.; Tassinari, C.C.G.; Ruberti, E.; Brilli, M. U-Pb ages, geochemistry, C-O-Nd-Sr-Hf isotopes and petrogenesis of the Catalão II carbonatitic complex (Alto Paranaíba Igneous Province, Brazil): Implications for regional-scale heterogeneities in the Brazilian carbonatite associations. *Int. J. Earth Sci.* **2017**, *106*, 1963–1989. [CrossRef]
6. Melluso, L.; Guarino, V.; Lustrino, M.; Morra, V.; de' Gennaro, R. The REE- and HFSE-bearing phases in the Itatiaia alkaline complex (Brazil), and geochemical evolution of feldspar-rich felsic melts. *Mineral. Mag.* **2017**, *81*, 217–250. [CrossRef]
7. Mitchell, R.H. Primary and secondary niobium mineral deposits associated with carbonatites. *Ore Geol. Rev.* **2015**, *64*, 626–641. [CrossRef]
8. Khromova, E.A.; Doroshkevich, A.G.; Sharygin, V.V.; Izbrodin, L.A. Compositional evolution of pyrochlore-group minerals in carbonatites of the Belaya Zima Pluton, Eastern Sayan. *Geol. Ore Depos.* **2017**, *59*, 752–764. [CrossRef]
9. Hogarth, D.D. Classification and nomenclature of the pyrochlore group. *Am. Mineral.* **1977**, *62*, 403–410.
10. Atencio, D.; Andrade, M.B.; Christy, A.G.; Gieré, R.; Kartashov, P.M. The pyrochlore supergroup of minerals: Nomenclature. *Can. Mineral.* **2010**, *48*, 673–698. [CrossRef]
11. Christy, A.G.; Atencio, D. Clarification of status of species in the pyrochlore supergroup. *Mineral. Mag.* **2013**, *77*, 13–20. [CrossRef]
12. Guowu, L.; Guangming, Y.; Fude, L.; Ming, X.; Baoming, P.; de Fourestier, J. Fluorcalciopyrochlore, a new mineral species from Bayan Obo, Inner Mongolia, P.R. China. *Can. Mineral.* **2016**, *54*, 1285–1291. [CrossRef]
13. Timofeev, A.; Williams-Jones, A.E. The origin of niobium and tantalum mineralization in the Nechalacho REE Deposit, NWT, Canada. *Econ. Geol.* **2015**, *110*, 1719–1735. [CrossRef]
14. Moller, V.; Williams-Jones, A.E. Petrogenesis of the Nechalacho layered suite, Canada: Magmatic evolution of a REE-Nb-rich nepheline syenite intrusion. *J. Petrol.* **2016**, *57*, 229–276. [CrossRef]
15. Dumanska-Slowik, M.; Pieczka, A.; Tempesta, G.; Olejniczak, Z.; Heflik, W. "Silicified" pyrochlore from nepheline syenite (mariupolite) of the Mariupol Massif, SE Ukraine: A new insight into the role of silicon in the pyrochlore structure. *Am. Mineral.* **2014**, *99*, 2008–2017. [CrossRef]
16. Siegel, K.; Vasyukova, O.V.; Williams-Jones, A.E. Magmatic evolution and controls on rare metal-enrichment of the Strange Lake A-type peralkaline granitic pluton, Québec-Labrador. *Lithos* **2018**, *308–309*, 34–52. [CrossRef]
17. Kovalenko, V.I.; Yarmolyuk, V.V.; Kartashov, P.M.; Kozlovskii, A.M.; Listratova, E.N.; Salnikova, E.B.; Kovach, V.P.; Kozakov, I.K.; Kotov, A.B.; Yakovleva, S.Z.; et al. The Khaldzan-Buregtei massif of peralkaline

rare-metal igneous rocks: Structure, geochronology, and geodynamic setting in the caledonides of Western Mongolia. *Petrology* **2004**, *12*, 412–436.
18. Yin, J.; Li, G.; Yang, G.; Ge, X.; Xu, H.; Wang, J. Fluornatropyrochlore, a new pyrochlore supergroup mineral from the Boziguoer rare earth element deposit, Baicheng County, Akesu, Xinjiang, China. *Can. Mineral.* **2015**, *53*, 455–460. [CrossRef]
19. Archangel'skaya, V.V.; Ryabtsev, V.V.; Shuriga, T.N. Geological structure and mineralogy of the tantalum deposits of Russia. In *Mineral Commodities*; PH VIMS: Moscow, Russia, 2012; Volume 25, p. 318. (In Russian)
20. Sklyarov, E.V.; Gladkochub, D.P.; Kotov, A.B.; Starikova, A.E.; Sharygin, V.V.; Velikoslavinsky, S.D.; Larin, A.M.; Mazukabzov, A.M.; Tolmacheva, E.A.; Khromova, E.A. Genesis of the Katugin rare-metal ore deposit: Magmatism versus metasomatism. *Russ. J. Pac. Geol.* **2016**, *35*, 9–22. [CrossRef]
21. Donskaya, T.V.; Gladkochub, D.P.; Sklyarov, E.V.; Kotov, A.B.; Larin, A.M.; Starikova, A.E.; Mazukabzov, A.M.; Tolmacheva, E.V.; Velikoslavinski, S.D. Genesis of the Paleoproterozoic rare-metal granites of the Katugin Massif. *Petrology* **2018**, *26*, 47–64. [CrossRef]
22. Gladkochub, D.P.; Donskaya, T.V.; Sklyarov, E.V.; Kotov, A.B.; Vladykin, N.V.; Pisarevsky, S.A.; Larin, A.M.; Salnikova, E.B.; Saveleva, V.B.; Sharygin, V.V.; et al. The unique Katugin rare-metal deposit (southern Siberia): Constraints on age and genesis. *Ore Geol. Rev.* **2017**, *91*, 246–263. [CrossRef]
23. Savelieva, V.B.; Bazarova, E.P.; Khromova, E.A.; Kanakin, S.V. Rare-earth minerals in rocks of the Katugin rare-metal deposit (East Transbaikalia): Behavior of lanthanides and Y during crystallization of the saturated-in-fluorine agpaitic melt. *Zap. RMO (Trans. RMS)* **2017**, *146*, 1–21. (In Russian)
24. Kotov, A.B.; Vladykin, N.V.; Larin, A.M.; Gladkochub, D.P.; Salnikova, E.V.; Sklyarov, E.V.; Tolmacheva, E.V.; Donskaya, T.V.; Velikoslavinsky, S.D.; Yakovleva, S.Z. New data on the age of ore formation in the unique Katugin rare-metal deposit (Aldan Shield). *Dokl. Earth Sci.* **2015**, *463*, 663–667. [CrossRef]
25. Bykov, Y.V.; Archangel'skaya, V.V. Katugin rare-metal deposit. In *Transbaikalian Deposits*; Geoinformmark: Chita-Moscow, Russia, 1995; Volume 1, pp. 76–85. (In Russian)
26. Archangel'skaya, V.V.; Kazanskii, V.I.; Prokhorov, K.V.; Sobachenko, V.N. Geological structure, zoning and conditions of formation of the Katugin Ta-Nb-Zr deposit (Chara-Udokan district, East Siberia). *Geol. Ore Depos.* **1993**, *35*, 115–131.
27. Ryabtsev, V.V.; Chistov, I.V.; Shuriga, T.N. Tantalum ores of Russia: State and prospects of the development of the raw mineral base. In *Mineral Commodities*; PH VIMS: Moscow, Russia, 2006; Volume 21, p. 92. (In Russian)
28. Savelieva, V.B.; Bazarova, E.P.; Khromova, E.A.; Kanakin, S.V. Fluorides and fluorcarbonates in rocks of the Katugin complex, Eastern Siberia: Indicators of geochemical mineral formation conditions. *Geol. Ore Depos.* **2017**, *59*, 561–574. [CrossRef]
29. Starikova, A.E.; Sklyarov, E.V.; Sharygin, V.V. Y-REE Mineralization in Biotite-Arfvedsonite Granites of the Katugin Rare-Metal Deposit, Transbaikalia, Russia. *Dokl. Earth Sci.* **2019**, *487*, 800–803. [CrossRef]
30. Larin, A.M.; Kotov, A.B.; Vladykin, N.V.; Gladkochub, D.P.; Kovach, V.P.; Sklyarov, E.V.; Donskaya, T.V.; Velikoslavinskii, S.D.; Zagornaya, N.Y.; Sotnikova, I.A. Rare metal granites of the Katugin complex (Aldan Shield): Sources and geodynamic formation settings. *Dokl. Earth Sci.* **2015**, *464*, 889–893. [CrossRef]
31. Podkovyrov, V.N.; Kotov, A.B.; Larin, A.M.; Kotova, L.N.; Kovach, V.P.; Zagornaya, N.Y. Sources and provenances of lower Proterozoic terrigenous rocks of the Udokan Group, Southern Kodar-Udokan depression: Results of Sm-Nd isotopic investigations. *Dokl. Earth Sci.* **2006**, *408*, 518–522. [CrossRef]
32. Prokhorov, K.V.; Sobachenko, V.N. Structural, petrological and geochemical conditions of the formation of ore-bearing high-temperature sodic metasomatites. In Proceedings of the Inner Structure Ore-Bearing Precambrian Faults, Moscow, Russia, 1985; pp. 94–121. (In Russian).
33. Huang, H.; Wang, T.; Zhang, Z.; Li, C.; Qin, Q. Highly differentiated fluorine-rich, alkaline granitic magma linked to rare metal mineralization: A case study from the Boziguo'er rare metal granitic pluton in South Tianshan Terrane, Xinjiang, NW China. *Ore Geol. Rev.* **2018**, *96*, 146–163. [CrossRef]
34. Bonazzi, P.; Bindi, L.; Zoppi, M.; Capitani, G.C.; Olmi, F. Single-crystal diffraction and transmission electron microscopy studies of "silicified" pyrochlore from Narssârssuk, Julianehaab district, Greenland. *Am. Mineral.* **2006**, *91*, 794–801. [CrossRef]
35. Chakhmouradian, A.R.; Mitchell, R.H. New data on pyrochlore- and perovskite-group minerals from the Lovozero alkaline complex, Russia. *Eur. J. Mineral.* **2002**, *14*, 821–836. [CrossRef]
36. Williams, C.T.; Wall, F.; Woolley, A.R.; Phillipo, S. Compositional variation in pyrochlore from the Bingo carbonatite, Zaire. *J. Afr. Earth Sci.* **1997**, *25*, 137–145. [CrossRef]

37. Hogarth, D.D. Pyrochlore, apatite and amphibole: Distinctive minerals in carbonatite. In *Carbonatites: Genesis and Evolution*; Unwin Hyman: London, UK, 1989; pp. 105–148.
38. Voloshin, A.V.; Pakhomovskiy, Y.A.; Pushcharovskiy, D.Y.; Nadezhina, T.N.; Bakhchisaraitsev, A.Y.; Kobyashev, Y.S. Strontiopyrochlore: Composition and structure. *Tr. Mineral. Muzeya AN SSSR* **1989**, *36*, 12–24. (In Russian)
39. Levashova, E.V.; Skublov, S.G.; Marin, Y.B.; Lupashko, T.N.; Ilchenko, E.A. Trace elements in zircon from rocks of the Katugin rare-metal deposit. *Geol. Ore Depos.* **2015**, *57*, 579–590. [CrossRef]
40. Lumpkin, G.R.; Ewing, R.C. Geochemical alteration of pyrochlore group minerals: Pyrochlore subgroup. *Am. Mineral.* **1995**, *80*, 732–743. [CrossRef]
41. Torro, L.; Villanova, C.; Castillo, M.; Goncalves, A.O.; Melgarejo, J.C. Niobium and rare earth minerals from the Virulundo carbonatite, Namibe, Angola. *Mineral. Mag.* **2012**, *76*, 393–409. [CrossRef]
42. Starikova, A.E.; Sharygin, V.V.; Sklyarov, E.V. Ba-dominant fluoroaluminates from the Katugin rare-metal deposit (Transbaikalia, Russia). *Dokl. Earth Sci.* **2017**, *472*, 67–71. [CrossRef]